



Geochemistry of the upper Han River basin, China, 1: Spatial distribution of major ion compositions and their controlling factors

Siyue Li ^{a,b}, Quanfa Zhang ^{a,*}

^a Center for Watershed Ecology, Wuhan Botanical Garden, The Chinese Academy of Sciences, Wuhan 430074, China

^b Graduate School of the Chinese Academy of Sciences, Beijing 100049, China

ARTICLE INFO

Article history:

Received 9 January 2008

Accepted 14 August 2008

Available online 31 August 2008

Editorial handling by R.M. Price

Keywords:

Upper han river

Major ion chemistry

Geochemistry

Water quality

ABSTRACT

The upper Han River basin (approximately 95,200 km²) is the water source area of China's South-to-North Water Transfer Project. Over the period from 2005 to 2006, a total of 292 grab samples collected from 47 sites in the upper Han River were analyzed for major ions (Cl⁻, NO₃⁻, SO₄²⁻, HCO₃⁻, Na⁺, K⁺, Ca²⁺ and Mg²⁺), Si, T, pH, EC and TDS. Correlation matrix and principal component analysis were used to quantify the geochemical and anthropogenic processes and identify factors influencing the ionic concentrations. The results reveal that the waters are slightly alkaline with low ionic strength, and all ions show remarkable spatial variations. The lowest solute concentrations are observed in catchment with higher vegetation cover, with higher Cl⁻, NO₃⁻ and SO₄²⁻ concentrations occur in catchments with industrial establishments. The major ion chemistry of the upper Han River basin is mainly controlled by rock weathering with HCO₃⁻ and Ca²⁺ dominating the major ion composition. The spatial variation in overall water quality as well as comparison with WHO and Chinese standards for drinking water indicates that the basin has high-water quality, yet it is possible that NO₃⁻ enrichment will occur in the near future. This research will help water conservation in the basin for the interbasin water transfer project.

© 2008 Elsevier Ltd. All rights reserved.

1. Introduction

Water quality has been rapidly declining worldwide particularly in developing countries due to natural and anthropogenic processes (Carpenter et al., 1998; Chen et al., 2002). The major element chemistry of many of the world's major rivers has been studied, notably the Amazon (Gibbs, 1972; Stallard and Edmond, 1981; 1983; 1987), the Ganges–Brahmaputra (e.g., Sarin et al., 1989), the Lena (Gordeev and Sidorov, 1993; Huh et al., 1998a,b), and the Godavari (Biksham and Subramanian, 1988). The study of stream geochemistry reveals the pattern and linkage between evaporation, chemical weathering, precipitation and anthropogenic impacts (Gibbs, 1970; Meybeck, 1987; Brennan and Lowenstein, 2002). Quantifying the major ion composition of stream waters also has broad implica-

tions, *i.e.*, water quality type, hydrogeology characteristics, weathering processes and rainfall chemistry (Brennan and Lowenstein, 2002; Cruz and Amaral, 2004).

In China, reports on major ion chemistry have focused on the Yellow River (Hu et al., 1982; Li and Zhang, 2005; Zhang et al., 1990, 1995) and the Changjiang River (Hu et al., 1982; Zhang et al., 1990; Chen et al., 2002; Li and Zhang, 2005). The earliest study on major ion chemistry of the Han River was reported by Hu et al (1982) but with a low sampling frequency at few stations. Chen et al (2002) studied the water chemistry of the Changjiang River and its tributaries, including the Han River and reported a significant increasing trend in SO₄²⁻ concentrations in the Changjiang River due to anthropogenic inputs. However, the study only had data from 11 sites on the main channel of the upper Han River, which is hardly sufficient for characterizing the major ion chemistry of the vast Han River drainage basin. Thus, systematic hydrochemical information on the Han River, a main tributary of the Changjiang

* Corresponding author. Tel.: +86 27 87510702; fax: +86 27 87510251.
E-mail address: qzhang@wbgcas.cn (Q. Zhang).

River, is unavailable, which represents a significant gap in the understanding of river chemistry, physical and chemical weathering, and elemental cycles at local and global scales.

The upper Han River basin is the water source area of China's South-to-North Water Transfer Project that diverts water to North China for domestic, industrial and irrigational usages. Thus, its water quality is of great concern. Previous studies have reported its nutrient concentrations and metal contamination (Li et al., 2008a,b,c), and an increasing trend of Cl^- and SO_4^{2-} concentrations in the basin (Chen et al., 2002). In this study, an extensive analysis has been conducted to determine the spatial patterns of major ion composition, and to identify their sources and their controlling factors.

2. Site description and methods

2.1. Upper Han River basin

The upper Han River basin with an elevation from 210 to 3500 m, has a drainage area of 95, 200 km² and is

approximately 925 km long (Fig. 1; Li et al., 2008a). Climate in the basin can be considered as north sub-tropic monsoon, and its annual mean temperature ranges between 12 and 16 °C (Li et al., 2008b). Average annual precipitation is from 700–1800 mm, and as much as 80% is concentrated in the period from May to October (Li et al., 2008a). The area has an average potential evaporation of about 900–1500 mm/a and its annual water balance seems to show a water deficit (Zhang et al., 1996). The average runoff is about $41.1 \times 10^9 \text{ m}^3/\text{a}$, accounting for 70% of the total runoff of the entire basin (Li et al., 2008a, b).

The lithology of the upper Han River basin is composed of granites, granitic gneisses, quartzites, sandstones, shales, schist and limestones (Zhang et al., 1996), with carbonates particularly abundant in the basin (Chen et al., 2002). In the catchment strata of the Sinian (Neoproterozoic), Cambrian, Ordovician, Silurian, Devonian, Carboniferous, Permian, Cretaceous, Tertiary and Quaternary are exposed (Zhang et al., 1996). The basin is comprised of hills, mounds and valley catchments (Fig. 1; Zhang et al., 1996). The soils in this area are formed from parent rocks such as clay, phyllites, shales and schists.

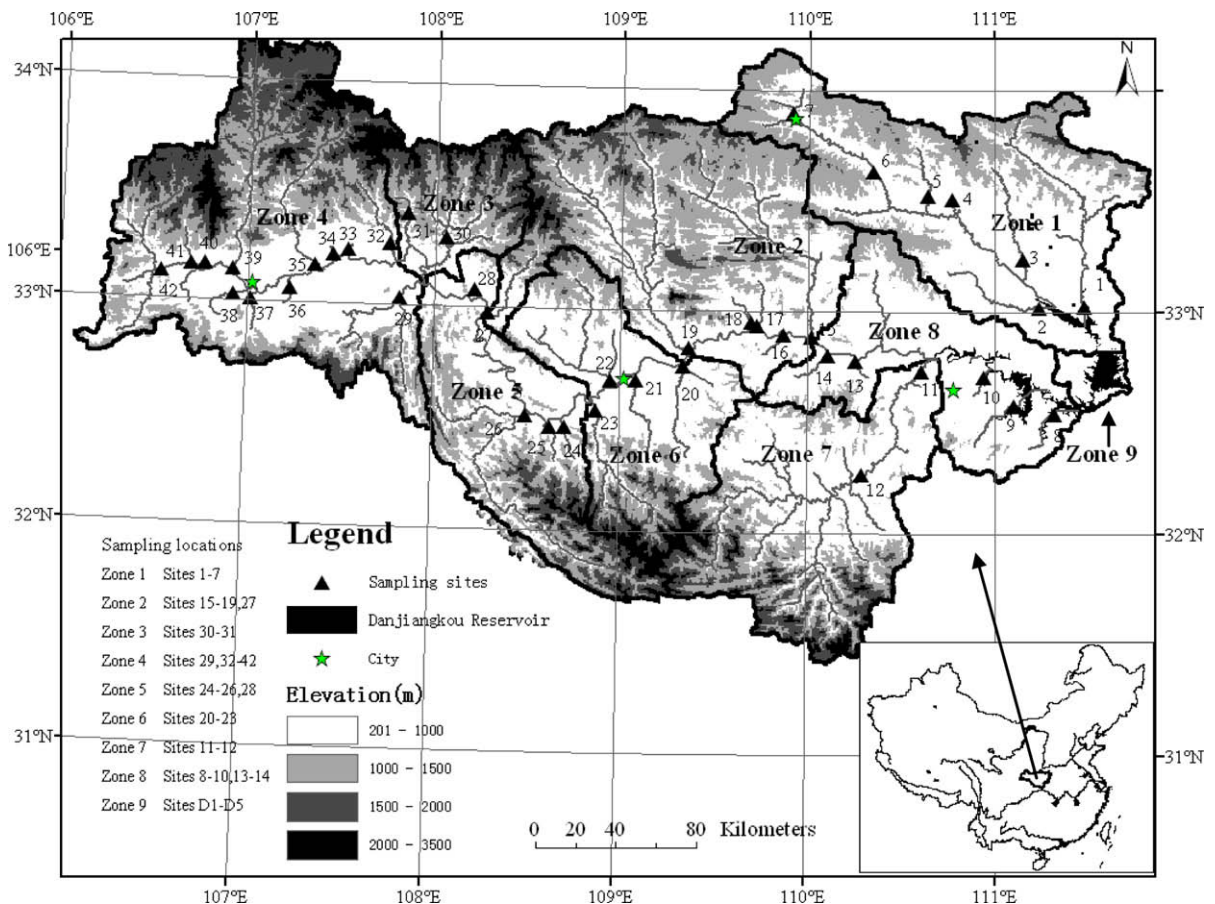


Fig. 1. The upper Han River basin showing the sampling sites, DEM and drainage system, China (Zone 1 – Dan River, Zone 2 – South of the Qinling Mountains, Zone 3 – Ziwu River, Zone 4 – Hanzhong Plain, Zone 5 – North of the Daba Mountains, Zone 6 – Ankang Plain, Zone 7 – Du River, Zone 8 – Danjiangkou Reservoir Catchment and Zone 9 – Danjiangkou Reservoir, Table 2).

2.2. Sampling and analysis

A total of 292 grab samples were collected from 47 sites in the upper Han River basin including the Danjiangkou Reservoir (Fig. 1; Table 1). Field surveys, according to hydrologic regime, were conducted in June, August and November 2005, and April, June and October 2006 for rivers, and in November 2004, January, April, June, August and November 2005, and April and June 2006 for the Reservoir. Of which, August and November in 2005 and October in 2006 were rainy season, and the rest were dry season, therefore, there are a total of 136 water samples in the rainy season, with 156 samples in the dry season. Water samples were collected from approximately 10 cm (1 m in the Reservoir) below the surface using previously acid-washed high-density polyethylene (HDPE) 1 L bottles. All the samples were filtered (0.45 µm Millipore nitrocellulose filter) in the field and a small portion of these samples was stored for measuring Cl^- , NO_3^- and SO_4^{2-} , while another portion was acidified with ultra-pure HNO_3 to pH < 2 for Na, K, Ca, Mg and Si determination. They were stored at 4 °C in HDPE bottles. Cleaning of plastic bottles and plastic bags was carried out by soaking in 15% (v/v) HNO_3 for 24 h and then rinsing with milli-Q water.

Water temperature, pH, electrical conductivity (EC) and total dissolved solids (TDS) were measured in situ using a YSI 6920, which had been calibrated before use. The HCO_3^- was determined by titration with HCl on the day of sampling. Major cations (Na, K, Ca and Mg) and Si were determined using Inductively Coupled Plasma Atomic Emission Spectrometry (ICP-AES) (IRIS Intrepid II XSP DUO, USA). Anions (Cl^- , NO_3^- and SO_4^{2-}) were measured using a Dionex Ion Chromatograph (IC) (Dionex Corpora-

tion, Sunnyvale, CA, USA). Reagent and procedural blanks were determined in parallel to the sample treatment using identical procedures. Each calibration curve was evaluated by analyses of quality control standards before, during and after the analyses of a set of samples. The analytical precision was within 10%, 95.6% for Ca, 103.7% for Mg, 94.3% for Na, 96.8% for K and 98.2% for Si using ICP-AES, 98.6% for SO_4^{2-} , 97.2% for Cl^- , 96.4% for NO_3^- using IC, and 98.0% for HCO_3^- , respectively.

2.3. Classification of the basin by watershed

The upper Han River basin was divided into nine zones through integrated watershed delineation by DEM, watershed characteristic, landscape, geology and human activities (O'Callaghan and Mark, 1984; Cai et al., 2000; Li et al., 2008a; Fig. 1; Table 1). There are industrial cities, i.e., Shangluo, Hanzhong, Ankang and Shiyan in zones 1, 4, 6 and 8, respectively (Fig. 1). Landsat Thematic Mapper (TM; 28.5 m resolution) imagery from 2000 was used to map land use/land cover in the basin (Shen et al., 2006). Five land use and land cover types, i.e., vegetated land, agriculture, urban, waters, and bare lands, were delineated in this study (Li et al., 2008a).

2.4. Statistical analysis

Pearson correlation analysis for subwatershed averages was carried out to evaluate the relationships between various physiochemical parameters, with statistical significance set at $p < 0.05$. Factor analysis was carried out to reveal the underlying structure of the dataset by means of distance between variables in a multi-dimensional

Table 1
Descriptions of zones in the upper Han River basin, China

Zone	Subwatershed	Watershed description			
<i>(a) Watershed description</i>					
1	Dan River	Intensive human influence including agriculture in buffer zone and mineral exploration, with large landscape variation			
2	South of the Qinling Mountains	A forested area with lowest urbanization and serious soil erosion			
3	Ziwu River	A forested area including coniferous upland with little human influences, showing granite geology			
4	Hanzhong Plain	The primary agricultural area, with higher urbanization (Hanzhong city)			
5	North of the Daba Mountains	A primary area for minerals with relative higher agricultural land area compared to the South of the Qinling Mountain			
6	Ankang Plain	The highest agriculture land use area, with intensive cultivation in buffer zones			
7	Du River	The largest catchment in the upper Han River basin			
8	Danjiangkou Reservoir Catchment	An industrial area (Shiyan city) where industrial effluents drain into the rivers			
9	Danjiangkou Reservoir	The important protected area, supplying water for North-China			
Basin-wide scale					
The average runoff is about $41.1 \times 10^9 \text{ m}^3/\text{year}$ in the upper stream, and $18 \times 10^9 \text{ m}^3/\text{year}$ in the down stream. The average rain fall decreases from upper to down stream					
Zone	Land use and land cover composition (%)				
	Vegetated land	Agriculture	Urban	Bare-land	Waters
<i>(b) Land use and land cover composition in subwatershed</i>					
Zone 1	78.45	12.37	0.33	8.29	0.55
Zone 2	85.68	10.07	0.04	3.80	0.41
Zone 3	95.68	3.41	0.08	0.48	0.36
Zone 4	80.54	17.15	1.20	0.45	0.66
Zone 5	83.17	15.00	0.19	0.65	1.00
Zone 6	77.21	21.15	0.25	0.84	0.55
Zone 7	85.08	13.45	0.28	0.59	0.60
Zone 8	77.02	11.83	0.59	7.68	2.88

space. Principal component analysis (PCA) with Varimax rotation was used for extraction and deriving factor derivation (Stallard and Edmond, 1987; Cruz and Amaral, 2004). All the processes were performed using SPSS 13.0.

3. Results

Major-ion compositions are given in Table 2. Waters are slightly alkaline, with an average pH ranging from 8.0 to 8.4. Lower values are attained in Zones 4 and 8. Stream waters have low TDS, from 110 to 227 mg/L and low mineralization, as shown by the EC measurements, varying from 168 to 349 $\mu\text{S}/\text{cm}$ (Table 2). EC has strong positive correlation with TDS ($R = 1$, $p < 0.01$) (Table 3), and their lowest values are observed in Zone 3 (Table 2).

Calcium and magnesium are the most abundant cations with average concentrations of 24.1–44.9 and 3.5–12.5 mg/L, respectively (Table 2). Potassium is the least abundant major cation with an average content of 0.8–1.7 mg/L. Bicarbonate is the most abundant major anion, and its averages range from 97.5 to 180 mg/L. The second most abundant anion is SO_4^{2-} ranging from 15.5 to 50.6 mg/L, and the mean contents of Cl^- and NO_3^- are nearly equal. All the major ions show obvious spatial variations, and anions and the most abundant cations (Ca^{2+} and Mg^{2+}) generally display their lowest values in Zone 3 (Table 2). Silicon has lower concentration with a median value of 3.99 mg/L, and it is lowest in Zone 9 (Table 2).

Calcium the dominant cation, contributes 59.4–86.6% to the major-cation budget. Anion chemistry was dominated by HCO_3^- constituting from 50.0% to 90.1% of the major anions with few exceptions. Thus, water composition is dominated by HCO_3^- and Ca^{2+} . Calcium and Mg^{2+} together account for 69.7–97.4% of the cations measured, while the sum of HCO_3^- and SO_4 comprise 69.9–98.4% of the anions (Fig. 2).

Relationships between measured components at sub-watershed scale were examined (Table 3). Bicarbonate, Ca^{2+} and Mg^{2+} show positive correlations ($R > 0.89$, $p < 0.01$), and their significant contribution to the overall chemical composition of waters is shown by their correlations with TDS ($R > 0.88$, $p < 0.01$). Chloride and Na^+ are positively correlated ($R = 0.88$, $p < 0.01$), and their contributions to the hydrochemistry is shown by the correlation between Na and TDS ($R = 0.72$, $p < 0.05$). Potassium only shows significant correlation with Na^+ (Table 3).

Factor analyses on physico-chemical parameters derive three significant factors with eigenvalue > 1.0 (Table 4). The results indicate three components accounting for about 71% of the total variability. The scores of variables on the principal component axis are plotted in Fig. 3, which shows the similarities between variables in the dataset.

4. Discussion

4.1. Spatial pattern of major ions

Significant spatial variations of major ions indicate the influence of anthropogenic activities and different lithology at subwatershed scale (Chen et al., 2002). For instance,

the Ziwu River generally has the lowest concentrations of hydrochemical variables (Table 2), and that may be explained by it having the highest vegetation coverage (Li et al., 2008a; Table 1) and granite lithology (Table 1). Positive correlations between Cl^- , NO_3^- and SO_4^{2-} ($R > 0.76$, $p < 0.05$) demonstrate their common sources and their spatial variations reveal the impacts of human activities indicated by their higher concentrations in subwatersheds with industrial establishments such as the Danjiangkou Reservoir catchment (Zone 8) (Tables 2 and 3).

PCA analysis (Table 4; Fig. 3) demonstrates the strong relationships between EC, TDS, Ca^{2+} , Mg^{2+} and HCO_3^- in the first component, reflecting carbonate weathering (Gibbs, 1972; Stallard and Edmond, 1987). The geochemical relationships between Na^+ , K^+ , Cl^- and SO_4^{2-} in the second component indicate the weathering of silicate and evaporite minerals, silicate contributes much more due to the minimal amount of evaporites in the basin (Chen et al., 2002; Cruz and Amaral, 2004). The third component shows the dominant nature of NO_3^- , which accounts for anthropogenic inputs, mineralization and atmospheric deposition.

Compared to major-ion compositions of the other large rivers in the world, the average TDS concentration in the upper Han River basin is relatively high, i.e., more than three times the global median of 65 mg/L (Table 5). Meanwhile there are dramatic increases in Cl^- and SO_4^{2-} concentrations, compared to the period of 1958–1990 (Chen et al., 2002). For instance, the SO_4^{2-} concentration has increased from less than 20 mg/L to approximately 32 mg/L with a maximum of 162 mg/L.

4.2. Mechanisms controlling the major-ion chemistry of the upper Han River basin

River solutes have multiple sources from physical, chemical and biological processes in the drainage basin. The major sources of dissolved salts in a river include sea salts carried by atmosphere and deposited in the river (cyclic salts); weathering of silicate, carbonate, evaporite and sulfide minerals; and anthropogenic causes. Their origins are discussed below.

4.2.1. Cyclic salts

Generally, Cl^- in surface waters with no terrestrial sources declines systematically with increasing distance from the sea (Stallard and Edmond, 1981). However, the reverse was observed by Chen et al (2002) in the Changjiang River due to a small contribution of cyclic salts to riverine dissolved salt loads. In this study, Cl^- concentration in the upper Han River, a tributary of the Changjiang River and more than a thousand of kilometers from the sea, is 6.23 mg/L (lower than 10 mg/L) at basin-wide scale. Elevated Cl^- concentrations are found in many rivers, i.e., the peak value is 70.7 mg/L (Table 2), therefore, high- Cl^- concentrations in the upper Han River basin most likely originate from weathering of evaporite rocks and anthropogenic sources rather than from the ocean.

4.2.2. Weathering

Gibbs (1970) provided a simple plot of TDS versus the weight ratio of $\text{Na}/(\text{Na} + \text{Ca})$ or $\text{Cl}/(\text{Cl} + \text{HCO}_3)$ to determine

Table 2

Water chemical data statistics: main variables (T, pH, TDS, EC), Si and major-ions composition in each subwatershed (unit in mg/L except T in °C, EC in µs/cm and pH)

		T	pH	TDS*	EC	Cl ⁻	NO ₃ ⁻	SO ₄ ²⁻	HCO ₃ ⁻	Na	K	Ca	Mg	Si
Zone1	Min	12.38	7.72	112.50	173.20	2.90	1.65	16.60	67.10	0.39	0.47	22.93	4.31	2.07
	Max	31.29	9.27	372.40	572.80	70.67	61.54	75.86	317.50	14.24	3.82	72.28	25.87	9.88
	Average	21.93(a)	8.33(a)	227.06(a)	349.31(a)	8.59(ab)	9.23(a)	36.80(b)	179.58(a)	4.99(a)	1.73(a)	43.45(ab)	12.48(a)	4.84(ab)
	SD	5.93	0.37	54.13	83.26	10.70	9.67	15.10	53.60	3.06	0.76	10.54	5.47	1.92
	Median	23.38	8.29	225.55	347.10	5.84	7.59	34.42	165.31	4.40	1.65	43.22	11.50	4.33
Zone2	Min	14.28	7.66	114.60	176.30	1.70	0.73	13.80	109.80	0.39	0.31	27.62	2.48	0.65
	Max	32.81	9.03	274.80	422.80	36.06	11.60	78.83	260.80	6.03	3.03	65.16	15.43	5.97
	Average	21.31(ab)	8.24(a)	213.81(a)	328.90(a)	6.20(bc)	5.05(bc)	37.66(b)	175.03(a)	2.71(bc)	1.11(b)	44.90(a)	9.18(b)	3.84(c)
	SD	5.87	0.28	37.18	57.14	5.71	2.59	16.41	37.72	1.35	0.61	8.39	3.20	1.17
	Median	19.23	8.24	221.30	338.25	4.68	4.69	33.02	178.12	2.51	0.92	43.67	9.57	3.98
Zone3	Min	13.07	8.10	72.40	111.40	0.65	1.02	11.50	63.44	0.35	0.61	16.05	1.89	2.38
	Max	27.78	8.74	151.10	232.40	2.89	4.09	20.77	151.10	3.33	3.64	36.06	5.40	5.71
	Average	20.17(ab)	8.36(a)	109.49(c)	168.43(c)	1.83(c)	2.40(c)	15.46(d)	97.45(d)	1.70(c)	1.51(ab)	24.10(d)	3.45(e)	3.90(c)
	SD	5.38	0.20	27.47	42.25	0.62	0.99	3.01	29.05	0.85	0.82	6.60	1.20	1.13
	Median	19.92	8.36	107.70	165.70	1.80	2.32	15.73	99.84	1.74	1.30	24.94	3.22	3.92
Zone4	Min	12.21	6.64	79.60	122.40	1.24	0.65	8.20	48.80	0.28	0.23	13.41	2.04	1.40
	Max	33.01	8.84	392.70	604.10	55.74	37.32	161.90	342.20	13.37	4.16	83.93	24.12	11.77
	Average	20.80(ab)	8.05(b)	181.32(b)	278.96(b)	5.45(c)	5.17(bc)	27.99(c)	147.98(b)	3.15(bc)	1.20(b)	38.72(b)	7.75(c)	4.98(a)
	SD	4.69	0.50	61.33	94.36	6.93	4.55	22.55	52.55	2.33	0.75	14.43	3.35	2.17
	Median	20.36	8.12	161.10	247.90	3.72	4.47	20.18	139.70	2.74	1.00	36.14	7.15	5.01
Zone5	Min	15.49	7.59	106.60	164.10	1.05	1.31	1.20	91.50	0.29	0.27	26.80	3.75	2.52
	Max	35.66	8.82	258.50	397.70	5.45	7.93	59.19	234.50	7.42	3.53	60.85	10.95	7.43
	Average	21.46(ab)	8.31(a)	166.56(b)	256.25(b)	2.78(c)	4.09(bc)	23.64(cd)	141.37(b)	2.30(bc)	1.08(b)	37.05(b)	6.40(cd)	3.93(c)
	SD	5.03	0.30	35.21	54.18	1.03	1.66	10.68	31.31	1.48	0.82	7.02	1.79	1.22
	Median	21.51	8.29	163.40	251.40	3.02	3.74	22.60	131.76	2.10	0.87	34.73	5.85	3.54
Zone6	Min	13.21	7.75	110.10	169.70	2.23	0.82	16.90	79.30	0.32	0.44	21.37	3.88	1.64
	Max	30.47	8.80	269.40	414.50	36.35	11.61	44.23	269.40	8.67	3.73	54.08	9.08	5.63
	Average	21.44(ab)	8.26(a)	168.23(b)	258.84(b)	5.87(bc)	5.03(bc)	30.17(bc)	137.25(b)	2.81(bc)	1.15(b)	34.40(bc)	6.49(cd)	3.64(c)
	SD	5.39	0.31	45.58	70.12	7.48	2.48	7.40	40.04	1.90	0.75	9.09	1.47	1.26
	Median	21.69	8.16	153.65	236.40	3.23	4.57	30.98	129.32	2.46	0.98	31.49	6.27	3.93
Zone7	Min	12.91	7.81	130.40	200.60	2.90	0.96	19.27	97.60	0.27	0.38	27.87	5.33	2.27
	Max	28.42	8.65	175.60	270.10	4.41	5.76	29.77	169.20	2.29	1.37	39.86	9.65	4.43
	Average	19.99(ab)	8.08(ab)	159.28(b)	245.11(b)	3.56(c)	3.89(bc)	23.89(cd)	132.99(bc)	1.58(c)	0.76(b)	33.50(bc)	6.74(cd)	3.47(c)
	SD	4.73	0.23	13.18	20.23	0.46	1.44	3.58	16.79	0.67	0.33	3.49	1.25	0.66
	Median	20.04	8.04	160.70	247.15	3.47	4.46	23.73	134.20	1.82	0.79	33.84	6.38	3.51
Zone8	Min	15.65	7.28	73.00	112.20	2.76	3.06	24.60	36.60	0.42	0.32	14.17	3.03	1.92
	Max	32.11	8.76	353.90	544.50	55.70	45.48	135.30	200.08	16.33	7.31	50.84	12.33	9.02
	Average	21.96(a)	8.01(b)	173.84(b)	267.53(b)	10.21(a)	7.08(ab)	50.61(a)	105.30(cd)	4.13(b)	1.74(a)	30.87(cd)	6.00(d)	4.75(ab)
	SD	5.53	0.38	66.09	101.62	11.76	7.78	30.07	43.31	3.93	1.53	10.73	2.35	1.44
	Median	19.15	7.97	156.00	240.20	6.03	5.31	39.80	97.60	3.22	1.34	30.15	5.65	4.77
Zone9	Min	7.96	7.64	149.90	230.70	3.43	3.25	21.21	92.72	0.51	0.44	29.57	5.27	1.05
	Max	30.52	8.85	291.20	448.00	11.41	10.81	45.29	213.50	6.15	2.59	54.22	16.89	4.06
	Average	19.02(bc)	8.23(a)	191.19(b)	292.29(b)	5.73(bc)	5.72(bc)	32.60(bc)	144.06(b)	3.48(b)	1.13(b)	39.77(b)	9.38(b)	2.53(d)
	SD	7.05	0.28	27.64	40.58	1.73	1.32	7.24	21.55	1.60	0.51	6.55	2.48	0.83
	Median	17.60	8.25	185.70	287.05	5.58	5.68	29.99	140.30	3.51	1.04	39.54	8.92	2.47
Upper Han River	Min	7.96	6.64	72.40	111.40	0.65	0.65	1.20	36.60	0.27	0.23	13.41	1.89	0.65
	Max	35.66	9.27	392.70	604.10	70.67	61.54	161.90	342.20	16.33	7.31	83.93	25.87	11.77
	Average	20.94	8.18	186.81	287.27	6.23	5.83	32.26	147.57	3.31	1.29	38.30	8.17	4.25
	SD	5.61	0.40	56.57	86.29	7.53	5.44	19.26	49.09	2.50	0.86	11.75	3.93	1.76
	Median	20.04	8.21	181.30	279.85	4.57	4.71	29.19	140.30	2.79	1.10	37.25	7.58	3.99

The different letters indicate statistical difference among zones at $p < 0.05$; LSD test.

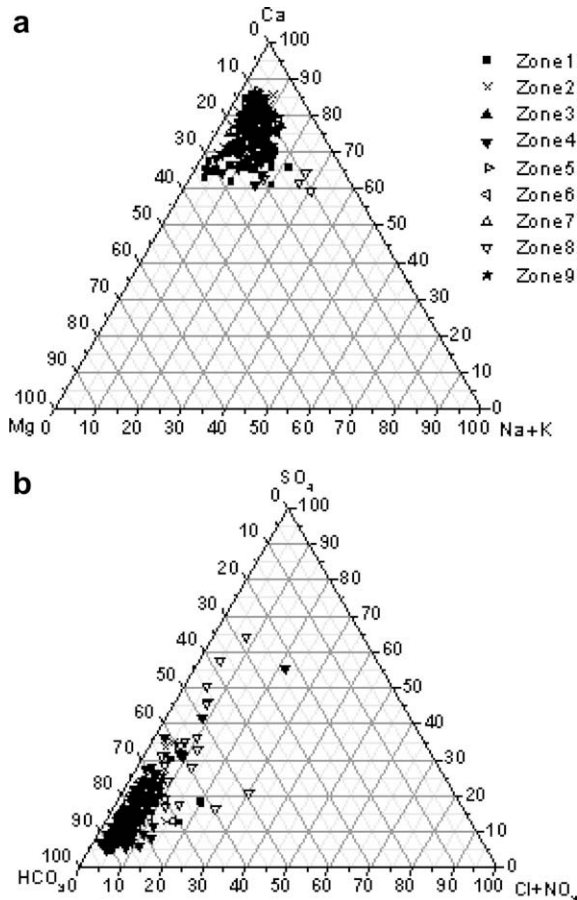
* TDS is determined by YSI6920.

Table 3Pearson correlation matrix for average chemical composition in subwatershed of the upper Han River basin, China ($n = 9$)

	T	pH	EC	TDS	Cl	NO ₃	SO ₄	HCO ₃	Na	K	Ca	Mg
T	1											
pH	-0.02	1										
EC	0.34	-0.05	1									
TDS	0.35	-0.05	1.00**	1								
Cl	0.53	-0.40	0.66	0.66	1							
NO ₃	0.49	-0.12	0.80*	0.80*	0.88**	1						
SO ₄	0.50	-0.45	0.64	0.64	0.95**	0.76*	1					
HCO ₃	0.22	0.23	0.88**	0.88**	0.26	0.51	0.21	1				
Na	0.45	-0.08	0.72*	0.72*	0.88**	0.96**	0.75*	0.40	1			
K	0.50	0.13	0.11	0.11	0.59	0.57	0.46	-0.16	0.69*	1		
Ca	0.18	0.07	0.94**	0.93**	0.37	0.56	0.37	0.96**	0.48	-0.16	1	
Mg	0.15	0.12	0.94**	0.94**	0.53	0.79*	0.43	0.89**	0.70*	0.12	0.89**	1

* Correlation is significant at the 0.05 level.

** Correlation is significant at the 0.01 level.

**Fig. 2.** Ternary diagrams showing cation (diagram a) and anion compositions (diagram b).

the relative importance of three major-natural mechanisms including atmospheric precipitation, evaporation and fractional crystallization, and rock weathering that control surface water chemistry. Plotting of TDS concentrations and the weight ratios of $\text{Na}/(\text{Na} + \text{Ca})$ for the upper Han River basin revealed that the river water is character-

Table 4

Results from the principal component analysis vectors, eigenvalues and cumulative variance

No.	Eigenvalue	Cumulative variance
1	5.400	44.999
2	1.733	14.442
3	1.365	11.376
4	0.810	6.746
5	0.710	5.919
6	0.664	5.533
7	0.518	4.319
8	0.363	3.023
9	0.291	2.429
10	0.075	0.629
11	0.058	0.487
12	0.012	0.099

Principal vectors in bold.

ized by a very low ratio of $\text{Na}/(\text{Na} + \text{Ca})$ and a moderate TDS concentration (187 mg/L) (Fig. 4), typical of rock-dominated rivers (Gibbs, 1970).

The rock dominance of the major-ion chemistry in the basin provides an insight of chemical weathering in the drainage basin, since weathering of different parent rocks (e.g., carbonates, silicates, and evaporites) yields different combinations of dissolved cations and anions to solution. For example, Ca^{2+} and Mg^{2+} originate from the weathering of carbonates, silicates and evaporites, Na^+ and K^+ from the weathering of evaporites and silicates, HCO_3^- from carbonates and silicates, SO_4^{2-} and Cl^- from evaporites, while silica exclusively sources from the weathering of silicates (Chen, 1987).

To probe the relative importance of different weathering regimes, ternary plots of major-ion compositions were constructed (Fig. 2). The ternary anion diagram shows that waters contain a high- HCO_3^- concentration with most sampling sites clustering towards the HCO_3^- apex. On the cation plot, samples fall in the cluster near the Ca^{2+} apex. Also, the concentration ratio of $\text{HCO}_3^-:\text{Cl} + \text{SO}_4:\text{Si}$ is 34.7:9.1:1 (Table 2) and there is no significant correlation between Si and HCO_3^- indicating that the contribution of silicate to HCO_3^- is not significant. Further the Ca/SO_4 ratio is >1 (Table 2), suggesting that H_2SO_4 does not replace H_2CO_3 as a source

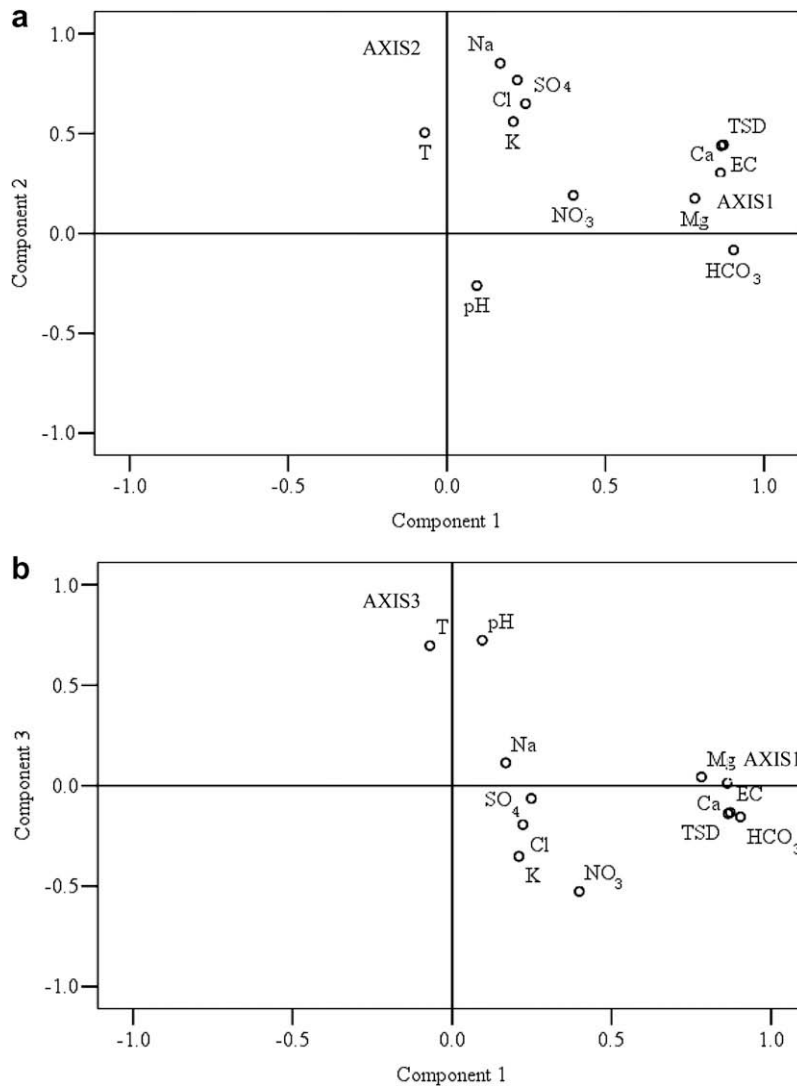


Fig. 3. Principal components analysis results for variables: (a) axis 1 vs. axis 2, and (b) axis 1 vs. axis 3.

Table 5

Comparisons of major-ion concentrations in the present study with other rivers

River	Cl ⁻	NO ₃ ⁻	SO ₄ ²⁻	HCO ₃ ⁻	Na ⁺ + K ⁺	Ca ²⁺	Mg ²⁺	Si	TDS	Reference
Upper Han River Bain	6.23	5.83	32.30	147.57	4.6	38.30	8.17	4.25	248 ^a	This study
Changjiang	2.9		11.7	133.8	8.3	34.1	7.6	2.89	205.9	Chen et al., 2002
Han River (main channel)	3.0		10.5	148.7	9.5	35.6	7.1	3.03	222.3	Chen et al., 2002
Yellow River	54.7		66.8	205.0	58.6	47.0	20.6		460	Chen et al., 2001
Zhujiang	1.2		7.7	132.0	2.2	38.4	4.5		192	
Amazon-Upper	6.5		7.0	68	7.5	19.1	2.3	5.18	122	Stallard and Edmond, 1983
Amazon-Lower	1.1		1.7	20	2.3	5.2	1.0	3.36	38	Stallard and Edmond, 1983
Ganga-Brahmaputra	6.0		14	163.7	16.8	28.1	11.9	4.43	196	Sarin et al., 1989
Lena	0.9		6.9	52.9	2.1	14.4	3.4	1.87	92	Huh et al., 1998b
Mackenzie	1.4		25.6	119	6.4	35.7	8.3	1.59	209	Chen et al., 2002
Orinoco	8.9		2.9	6.7	2.2	2.8	0.5	1.40	27	
Global Median	3.9		4.9	30.5	4.8	8.0	2.4		65	Meybeck and Helmer, 1989

^a The sum of major ions and Si.

of protons for rock weathering. Thus, major-ion chemistry of the upper Han River basin is dominated by carbonate

rock weathering. Meanwhile, the high ratios (>6) of alkaline earths (Ca + Mg)/alkalies (Na + K) and HCO₃⁻/alkalies

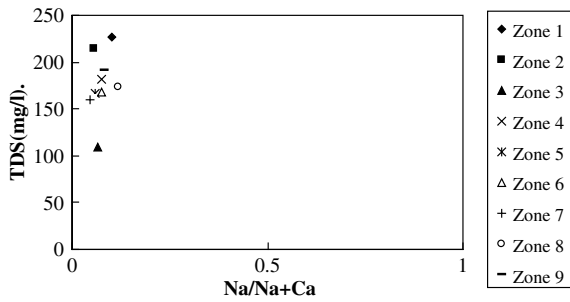


Fig. 4. The Gibbs graph of each subwatershed in the upper Han River basin, China.

ratios (Fig. 5), the molar Mg/Ca ratios, and the plots of HCO_3^- versus alkaline earths and their good positive correlations also point to the dominance of carbonate rock weathering, *i.e.*, calcite and dolomite are responsible for

water chemistry (Fig. 4; Dalai et al., 2002), consistent with the carbonate lithology in the catchment (Zhang et al., 1996; Cai et al., 2000).

Generally, K^+ and Na^+ in the waters are derived from evaporite dissolution and silicate weathering in rock weathering dominated rivers (Dalai et al., 2002). There are no significant correlations between Si and Na^+ , K^+ and HCO_3^- (Table 3), implying minimal weathering of silicate minerals in the basin. Moreover, consideration of the origins and cation exchange of Na^+ and K^+ , the biological uptake of K^+ , and the lithology of the basin, Na^+ and K^+ mainly derive from silicates. The strong correlations between Cl^- , SO_4^{2-} , Na^+ and K^+ also suggest they are sourced from the weathering of evaporites.

4.2.3. Anthropogenic causes

The major-ion chemistry can also be affected by human activities (Meybeck and Helmer, 1989). This impact has been increasing recently, due to the dramatic increases of industrial and agricultural activities. Though major-ion

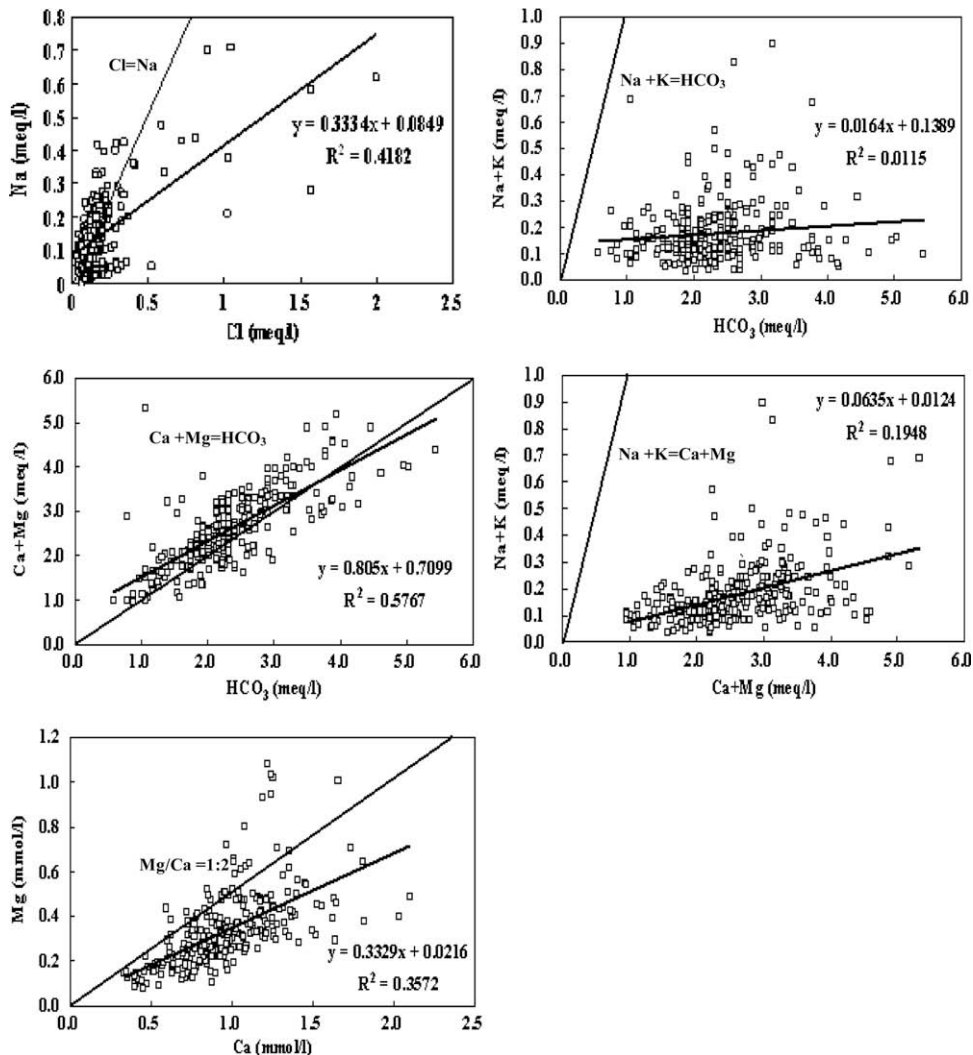


Fig. 5. Cl vs. Na, HCO_3^- vs. Na + K, HCO_3^- vs. Ca + Mg, Na + K vs. Ca + Mg and Mg vs. Ca plots for the upper Han River basin, China (in meq/L).

Table 6

Range in values of geochemical variables in waters and WHO (2006) and Chinese State Standard (CSS) for drinking water (unit: mg/L except pH, T in °C and EC in µs/cm)

Parameters	Upper Han River (Range)	Mean	WHO (2006)		CSS	Averages ^a
			Max desirable	Max permissible		
T	8.0–35.7	20.9	25			
pH	6.6–9.3	8.2	7.0–8.5	6.5–9.2	6.5–8.5	
EC	111.4–604.1	287.3	750	1500		
TDS	72.4–392.7	186.8	600	1000	1000	
HCO ₃ ⁻	36.6–342.2	147.6	300	600		58.4
SO ₄ ²⁻	8.2–161.9	32.3	250	600	250	11.2
Cl ⁻	0.7–70.7	6.2	250	600	250	7.8
NO ₃ ⁻	0.7–61.5	5.8	50	50	50	1.0
Na	0.3–16.3	3.3	50	200	200	6.3
K	0.2–7.3	1.3	100	250		2.3
Ca	13.4–83.9	38.3	75	250		15.0
Mg	1.9–25.9	8.2	30	150		4.1

^a Averages of world rivers (Levinson, 1974).

compositions on the basin-wide scale are within the range of natural water chemistry (Table 6), the abnormal peak values for Cl⁻, NO₃⁻ and SO₄²⁻ in some river samples (Table 2) are apparently due to anthropogenic sources (agrochemicals and industrial effluents).

Generally, NO₃⁻ has significantly higher concentrations compared to the average in world rivers (1 mg/L; Table 2; Levinson, 1974). This is mainly attributable to non-point pollutants, *i.e.*, agricultural fertilizers. Surficial geology, through rock weathering, is another important source for NO₃⁻ (Holloway *et al.*, 1998).

4.3. Quality assessment

Waters in the basin are of low mineralization with low hardness (Table 2). By comparing with the World Health Organization (WHO, 2006) and Chinese State Standards (CSS) (Chinese Ministry of Health, 2006) for drinking water (Table 6), all variables are within the maximum desirable limits except pH, NO₃⁻, HCO₃⁻ and Ca₂⁺, and they are only slightly over the maximum permissible limits. Chloride, Na⁺ and K⁺ have lower values compared to world averages (Tables 2 and 6).

Bicarbonate and Ca²⁺ have no known adverse effects on health. Only three samples for Ca²⁺ and two samples for HCO₃⁻ exceed the safe limits for drinking water, while they are all within the maximum permissible limits (Table 6). However, the peak content of NO₃⁻ exceeds the safe limit of 50 mg/L and its average is much greater than 1.0 mg/L (Table 6). High contents of NO₃⁻ can cause birth malformation, hypertension, high-iron haemoglobin and goiter. Also, excessive loading of NO₃⁻ contributes to river eutrophication (Carpenter *et al.*, 1998). In the present study, the peak value of NO₃⁻ Thus, there are indications of possible enrichment of NO₃⁻ beyond the maximum permissible limits for drinking water by the increasing anthropogenic activities in the basin (Wang *et al.*, 2006).

5. Conclusions

Waters in the upper Han River basin are slightly alkaline with low TDS and low mineralization. The drainage basin is typically carbonate, and river water in the basin has

largest relative abundances of HCO₃⁻ and Ca²⁺. With relatively low concentrations of Na⁺ and K⁺, the weathering of silicate minerals plays a less important role in determining the dissolved ions. Additionally, spatial variations of major-ion compositions at subwatershed scale indicate anthropogenic impacts, especially on Cl⁻, NO₃⁻ and SO₄²⁻.

The major-ion compositions on the basin-wide scale are within the range of natural water chemistry and also within the safe limits for drinking water standards. However, special attention should be paid to increases in the concentrations of Cl and SO₄ in the past 50 annum.

Acknowledgements

The research is supported by the National Key Technology R&D Program, PR China (2006BAC10B02), and the “Hundred-talent Project” of the Chinese Academy of Sciences (O629221C01). We would like to thank Sheng Gu, Jia Li, Lianfa Li, Sha Mu and Yiping Wang for their assistance with field sampling. The authors are grateful for the constructive comments of A.L. Ramanathan, an anonymous referee, and the handling editor.

References

- Biksham, G., Subramanian, V., 1988. Nature of solute transport in the Godavari basin, India. *J. Hydrol.* 103, 375–392.
- Brennan, S.K., Lowenstein, T.K., 2002. The major-ion composition of Silurian seawater. *Geochim. Cosmochim. Acta* 66, 2683–2700.
- Cai, S., Chen, G., Du, Y., Wu, Y., 2000. Thoughts on sustainable development in the Basin of Hanjiang River. *Resour. Environ. Yangtze Basin* 9, 411–418.
- Carpenter, S.R., Caraco, N.F., Correll, D.L., Howarth, R.W., Sharpley, A.N., Smith, V.H., 1998. Non-point pollution of surface waters with phosphorus and nitrogen. *Ecol. Appl.* 8, 559–568.
- Chen, J., 1987. *Water Environment Chemistry*. Higher Education Press, Beijing, China.
- Chen, J., Wang, F., Xia, X., Zhang, L., 2002. Major element chemistry of the Changjiang (Yangtze River). *Chem. Geol.* 187, 231–255.
- Chinese Ministry of Health, PR China., 2006. Chinese State Standards (CSS) for Drinking Water Quality, GB5749-2006.
- Cruz, J.V., Amaral, C.S., 2004. Major ion chemistry of groundwater from perched-water bodies of Azores (Portugal) volcanic archipelago. *Appl. Geochem.* 19, 445–459.
- Dalai, T.K., Krishnaswami, S., Sarin, M.M., 2002. Major ion chemistry in the headwaters of the Yamuna River system: chemical weathering, its temperature dependence and CO₂ consumption in the Himalaya. *Geochim. Cosmochim. Acta* 66, 3397–3416.

- Gibbs, R.J., 1970. Mechanisms controlling world water chemistry. *Science* 170, 1088–1090.
- Gibbs, R.J., 1972. Water chemistry of the Amazon River. *Geochim. Cosmochim. Acta* 36, 1061–1066.
- Gordeev, V.V., Sidorov, L.S., 1993. Concentrations of major elements and their outflow into the Laptev Sea by the Lena River. *Mar. Chem.* 43, 33–45.
- Holloway, J.M., Dahlgren, A., Hansen, B., Casey, W.H., 1998. Contribution of bedrock nitrogen to high nitrate concentrations in stream water. *Nature* 395, 785–788.
- Hu, M., Stallard, R.F., Edmond, J.M., 1982. Major ion chemistry of some large Chinese rivers. *Nature* 298, 550–553.
- Huh, Y., Panteleyev, G., Babich, D., Zaitsev, A., Edmond, J.M., 1998b. The fluvial geochemistry of the rivers of Eastern Siberia: II. Tributaries of the Lena, Omoloy, Yana, Indigirka/Kolyma, and Anadyr draining the collisional/accretionary zone of the Verkhoyansk and Cherskiy ranges. *Geochim. Cosmochim. Acta* 62, 2053–2075.
- Huh, Y., Tsoi, M.Y., Zaitsev, A., Edmond, J.M., 1998a. The fluvial geochemistry of the rivers of Eastern Siberia: I. Tributaries of the Lena River draining the sedimentary platform of the Siberian Craton. *Geochim. Cosmochim. Acta* 62, 1657–1676.
- Levinson, A.A., 1974. *Introduction to Exploration Geochemistry*, first ed. Applied Publishing Ltd., Wilmette, IL.
- Li, J., Zhang, J., 2005. Chemical weathering processes and atmospheric CO₂ consumption of Huanghe River and Changjiang River basins. *Chin. Geogr. Sci.* 15, 16–21.
- Li, S., Gu, S., Liu, W., Han, H., Zhang, Q., 2008a. Water quality in relation to the land use and land cover in the Upper Han River basin, China. *Catena* 75, 216–222.
- Li, S., Liu, W., Gu, S., Cheng, X., Xu, Z., Zhang, Q., 2008b. Spatio-temporal dynamics of nutrients in the upper Han River basin, China. *J. Hazard. Mater.* doi: 10.1016/j.jhazmat.2008.06.059.
- Li, S., Xu, Z., Cheng, X., Zhang, Q., 2008c. Dissolved trace elements and heavy metals in the Danjiangkou Reservoir, China. *Environ. Geol.* 55, 977–983.
- Meybeck, M., 1987. Global chemical weathering of surficial rocks estimated from river dissolved loads. *Am. J. Sci.* 287, 401–428.
- Meybeck, M., Helmer, R., 1989. The quality of rivers: from pristine stage to global pollution. *Palaeogeogr. Palaeoclimatol. Palaeoecol.* 75, 283–309.
- O'Callaghan, J.F., Mark, D.M., 1984. The extraction of drainage networks from digital elevation data. *Comput. Vision Graph. Image Process.* 28, 323–344.
- Sarin, M.M., Krishnaswamy, S., Dilli, K., Somayajulu, B.L.K., Moore, W.S., 1989. Major ion chemistry of Ganga–Brahmaputra river system: weathering processes and fluxes of the Bay of Bengal. *Geochim. Cosmochim. Acta* 53, 997–1009.
- Shen, Z., Zhang, Q., Yue, C., Zhao, J., Hu, Z., Lv, N., Tang, Y., 2006. The spatial pattern of land use/land cover in the water supplying area of the middle route of the south to north water diversion project. *Acta Geogr. Sin.* 61, 633–644.
- Stallard, R.F., Edmond, J.M., 1981. Geochemistry of the Amazon 1. Precipitation chemistry and the marine contribution to the dissolved load at the time of peak discharge. *J. Geophys. Res.* 86, 9844–9858.
- Stallard, R.F., Edmond, J.M., 1983. Geochemistry of the Amazon 2. The influence of geology and weathering environment on the dissolved load. *J. Geophys. Res.* 88, 9671–9688.
- Stallard, R.F., Edmond, J.M., 1987. Geochemistry of the Amazon 3. Weathering chemistry and limits to dissolved inputs. *J. Geophys. Res.* 92, 8293–8302.
- Wang, J., Yan, W., Jia, X., 2006. Modeling the export of point sources of nutrients from the Yangtze River basin and discussing countermeasures. *Acta Sci. Circum.* 24, 658–666.
- WHO, 2006. *Guidelines for Drinking-Water Quality*, third ed., vol.1 – Recommendations. World Health Organization, Geneva.
- Zhang, J., Huang, W., Letolle, R., 1995. Major element chemistry of the Huanghe, China Weathering processes and chemical fluxes. *J. Hydrol.* 168, 173–203.
- Zhang, J., Huang, W., Liu, M., 1990. Drainage basin weathering and major element transport of the Chinese rivers (Huanghe and Changjiang). *J. Geophys. Res.* 95, 13277–13288.
- Zhang, L., She, Z., Zhang, S., 1996. *Study of Chemical Elements in Water Environment*. Chinese Environment Science Press, Beijing, China.